RESEARCH ACTIVITIES III
Department of Electronic Structure

III-A Synthesis and Characterization of Exotic Molecule Based Nano-Crystals of Metal Acetylides: Toward Carbon Encapsulated Metal Dot Array, Metal Nano-Fibers and Hydrogen Storage

An anhydrous and oxygen-free condition has made us possible to obtain various transition metal-acetylides, where M = Fe, Co, Ni and so on. These acetylide compounds exhibit high potentiality for magnetic, catalytic, electronic, and gas adsorption functions. In contrast to explosive property of M_2C_2 type acetylides such as Ag_2C_2 and Cu_2C_2, CoC_2 and NiC_2 are rather stable in atmospheric condition. Thus, one can make the transition metal acetylides efficiently through the ion exchange reaction of metal chloride with CaC_2 in dehydrated acetonitrile solution. The MC_2 type compounds are expected to show CaC_2 type or MgC_2 type structure where metal cations and $C{\equiv}C^{2-}$ are alternatively stacked like a rock salt crystal, although the relative orientation of the anion molecule may depend on the synthetic condition. Annealing or heating above 300 ˚C induces the reduction of cations by anions, $C{\equiv}C^{2-}$ (charge neutralization), and resulting in the segregation of metal atoms by locating C_2 radicals outer and connecting C_2 bi-radicals as graphite-like or pyrolytic carbon shells. The relatively low segregation temperatures for FeC_2 and NiC_2 make it possible to draw metallic dots or wire circuits in MC_2 thin layers by scanning electron or VUV laser beams. The small size matrix MC_2 crystals prevent the strong dipole-dipole interaction between the metallic dots, while one can also wash out the matrix salt crystals by acid solution leaving the carbon encapsulated nano-metals on the base plate.

III-A-1 Manifestations of Ferromagnetism in CoC_2 by Water Coordination

NISHIJO, Junichi; OKABE, Chie; NISHI, Nobuyuki; SAWA, Hiroshi[1]
([1]KEK)

Due to the high absorbency of CoC_2, water molecules are coordinated to the Co^{2+} dication when CoC_2 is exposed to air or water. XRD pattern of the as-prepared anhydrous CoC_2, which is mostly originated from the scattering at the Co^{2+} dications, suggests the *fcc*-lattice of Co^{2+} with the lattice constants $a = b = 3.41$ Å and $c = 4.82$ Å. Judging from the crystal structures of CaC_2 and MgC_2, we expect that the Co^{2+} and C_2^{2-} ions form NaCl-like alternate stack, where the *fcc* arrangement of the Co^{2+} dications indicates the (static) orientation disorder of the C_2^{2-} dianions as shown in Figure 1. The cubic structure involving the orientation disorder of C_2^{2-} ions is also observed in CaC_2 at high temperature. Although CoC_2 is water-stable material unlike CaC_2 and MgC_2, absorbed water changes the crystal structure of CoC_2 drastically. After air-exposure, the XRD peaks become broad and the positions change as Co^{2+} cations form the body-centered-tetragonal sublattice with the lattice constants $a = b = 3.88$ Å, and $c = 3.40$ Å. In this phase, the *a*- and *b*-axes are expanded due to the absorbed waters coordinated to the Co^{2+}. The orientation of the C_2^{2-} dianions is also affected by the lattice expansion and/or steric hindrance of the water, resulting in the structural change from the isotropic disordered orientation (upper case in Figure 1) to anisotropic ordered orientation (lower case in Figure 1). Because the structural change is too drastic to be done in concert, a CoC_2 particle is divided into many small domains. Inter-molecular magnetic interaction is sensitive to the arrangement of the molecules. Therefore, it is expected that the magnetism of the hydrous and anhydrous CoC_2 are largely different. Figure 1 also shows the temperature dependence of the field-cooled magnetic susceptibilities χ of CoC_2 before and after the air-exposure,(a and b, respectively). χ of the anhydrous CoC_2 obeys the Curie-Weiss law in the high temperature range above *ca.* 70 K with Curie constant $C = 1.1$ emu·K/mol and anti-ferromagnetic (AF) Weiss temperature $\Theta = -10$ K, the former of which is obviously larger than the value of Co^{2+} cation ($C = 0.375$), suggesting the short-range strong ferromagnetic (FM) interaction. Although χ of the hydrous CoC_2 also obeys the Curie-Weiss law above 100 K, $C = 1.5$ emu·K/mol is significantly larger than that of anhydrous CoC_2 suggesting the expansion of the FM domain, while AF $\Theta = -3$ K indicates the weakening of the AF interaction between FM domains. The difference of the magnetism between hydrous and anhydrous CoC_2 is evidently caused by the water-induced structural changes; that is, the orientation ordering of C_2^{2-} and the expansion of the inter-chain distance. Judging from the fact that the interaction is weakened by lengthening the inter-molecular distance, it is concluded that the AF and FM interactions are attributed to the inter- and intra-chain interaction. In hydrous phase, where the FM interactions are connected each other and form the FM chain elongated parallel to the *c*-axis, resulting in the large FM domains.

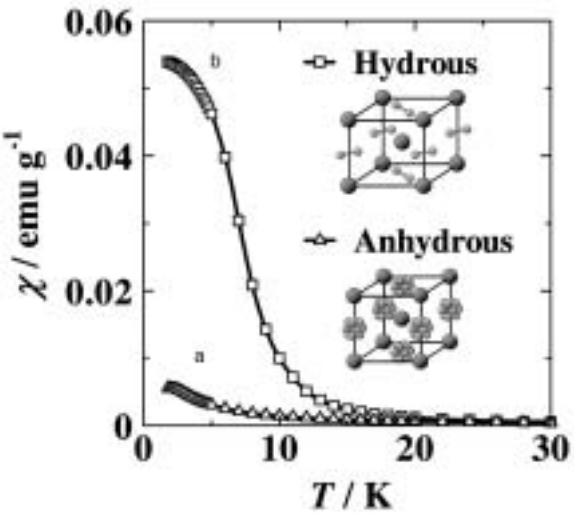

Figure 1. Temperature dependence of the field-cooled (10 Oe) magnetic susceptibilities χ of CoC_2 before and after the air-exposure,(a and b, respectively). Inserted are the structures that reproduce the XRD patterns of hydrous and anhydrous CoC_2 nano-crystals.

III-A-2 Molecule-Based Room Temperature Magnet: $(CoC_2)_2(H_2O)$ Nano-Rods

KOSUGI, Kentaroh; NISHIJO, Junichi; OKABE, Chie; BUSHIRI, Junaid M.; NISHI, Nobuyuki

As revealed in the previous study, CoC_2 crystals become ferromagnetic with coordinating water molecules to Co^{2+} ions. Elongation of the Co^{2+}–Co^{2+} distance makes the four-center interaction positive with the C_2^{2-} molecular axis perpendicular to the Co–Co axis. $(CoC_2)_2(H_2O)$ was synthesized from acetonitrile solution of $CoCl_2$ and suspended CaC_2 powder at 100 °C. The black product was washed by methanol with 5% of water. Figure 1 shows TEM images of the nano-rods. Figure 1-a indicates the presence of small particles with several nm radii in addition to the rod-like particles. Expanded in Figure 1-b is the lattice pattern of a rod exhibiting the long distances of the lattice stripes and wavy or somewhat disordered orientation of the atoms in the lattice sites. This kind of disorder is hardly seen in metal oxides or metallic particles with similar sizes. This is probably due to gradual hydration after the salt type crystals were formed, and thought to be characteristic of hydrophilic acetylide compounds. Figure 1-c shows the magnetic hysteresis curves of the particles at 300 K and 1.8 K. As seen from the curves, cohesive forces are as large as 780 Oe at 1.8 K and 650 Oe at 300 K. The magnetic saturation curve at 1.8 K suggests that the small spherical particles are superpara-magnetic at 300K and only the rod-type crystals behave as room temperature magnets.

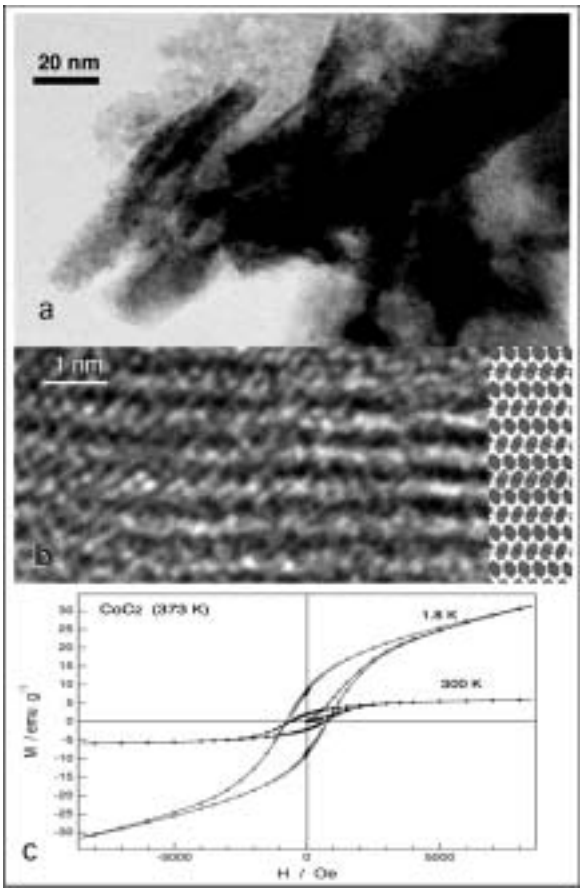

Figure 1. a: Transmission Electron Microscope image of the $(CoC_2)_2(H_2O)$ nano-rods that coexist with small spherical particles with several nm radii. b: Expanded view of a lattice image of a nano-rod. c: Magnetic hysteresis curves of CoC_2 synthesized at 100 °C.

III-A-3 Self-Assembled Nano-Wire Formation of Copper Acetylide (C_2Cu_2)

JUDAI, Ken; NISHIJO, Junichi; OKABE, Chie; NISHI, Nobuyuki

Copper acetylide (Cu–C≡C–Cu) was synthesized firstly for a long time ago, however, because of its explosive nature, the revealed properties are limited. From the view point of nano-science, the extreme small amount of explosive compound cannot achieve critical point of explosion, and is regarded as good candidate for source of copper or carbon in the dimension of nano-scale. The other side, recent progress of electron micros-copy makes it possible to uncover geometric structure of various compounds in atomic scale. We have examined synthesized copper acetylide by transmission electron microscopy (TEM), and its self-assembled nano-rod shape was discovered.

The copper acetylide was synthesized by the follow-ing recipe. First, 1 g of copper chloride (I), CuCl, was dissolved into 100 ml of 6% ammonia water. After 30 minutes of Ar gas bubbling in order to remove dissolved oxygen molecules, acetylene (C_2H_2) gas was bubbled in the solution.

$$2\,Cu^+ + C_2H_2 \rightarrow C_2Cu_2 + 2H^+$$

The color of the solution turned from blue (copper

ammine complex) into dark brown, and the product of C_2Cu_2 was precipitated. After 30 minutes reaction, the product was filtered and washed by water and methanol. Since this product contained excess solvent molecules, the estimation of the reaction yield was difficult. Very roughly, 50 ~ 100% of yield was guessed. For the measurement of TEM, small amount of the product was grinded and suspended in methanol. The methanol suspension was dropped onto a micro grid. After dry up, that grid was used as a specimen for TEM observation.

Figure 1 displays the TEM images of copper acetylide. Even if the copper acetylide synthesized in water solution was measured directly by TEM, nano-wires shaped with 5–20 nm of diameter and 200–800 nm in length were observed. This means that C_2Cu_2 in water solution is self-assembled into nano-sized rod structure. Due to the minimization of the electronic circuit on computer, production of nano-wires is one of the hottest topics in nano-technology. The various methods have been suggested for production ways of nano-wires, for example, nano-single crystal wire growth on nano-sized catalysis, deposition of metal on a template with nano-holes, and so on. The self-assembled method for nano-wire production is easily applied to mass-production and low-cost compared to the other method. The way of synthesis for nano-wire C_2Cu_2 is so simple that this is regarded as a remarkable way. Its crystal structure, aggregation mechanism, and physical properties (conductivity and so on) are still unclear in the present stage. In our group the theoretical calculation and various analysis techniques are in progress to reveal nature of copper acetylide nano-wire in detail.

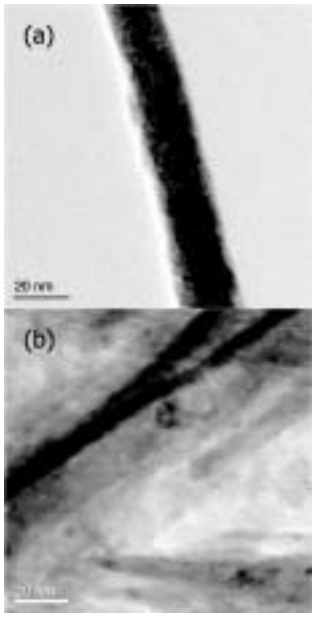

Figure 1. (a): Transmission Electron Microscope (TEM) image of copper acetylide (C_2Cu_2). 20 nm of rod diameter is one of the thickest wires. (b): . Typical TEM image of copper acetylide (C_2Cu_2). The bundle of nano-wires with 5 nm of diameter was observed.

III-A-4 Formation of Air Stable Carbon-Skinned Iron Nanocrystals from FeC_2

KOSUGI, Kentaroh; BUSHIRI, Junaid M.; NISHI, Nobuyuki

[*Appl. Phys. Lett.* **84**, 1753–1755 (2004)]

Charge neutralization reaction in ionic salt of $Fe^{2+}C_2^{2-}$ is found to produce carbon-skinned Fe nanocrystals. FeC_2 is formed as an intermediate product in the reaction of $FeCl_2$ solved in acetonitrile with CaC_2 fine powder and also able to be isolated as black nanocrystals. Heating of FeC_2 at temperature higher than 250 ºC induces segregation of metallic iron. The segregated carbons grow as graphitic sheets parallel to the growing Fe lattice plane. This direct bonding is due to an accidental matching of the Fe–Fe distance (2.866 Å) with that of the C_1–C_4 distance (2.842 Å) of the hexagonal rings in graphite. The X-ray diffraction pattern indicates that the particles are composed of α-Fe and graphitic carbon. The thickness of the skin is almost constant as thick as 3.5 nm independent of the body size. The particles with an average size of 30 nm exhibit temperature dependence of the magnetic cohesive force as function of $T^{-0.275}$.

III-B States of Neutral and Ionic Molecular Associates in Solutions

States of molecular associates particularly in aqueous solutions are of great importance in understanding the role of molecules in living organisms. We found that any ideally mixed state cannot be seen in protic-protic mixtures such as water-alcohol, water-acetic acid, and alcohol-acetic acid systems on the molecular level at solute molar fractions (χ_A) higher than 0.001. In such a system, solute-solute asociation is highly favored resulting in microscopic phase separation. In this year, we studied the aqueous mixture of hexafluoro-2-propanol (HFIP), and have shown that that structural transition of solvent clusters takes place at $x_{HFIP} \sim 0.1$ from the tetrahedral-like hydrogen bonded network of water at $x_{HFIP} \leq \sim 0.1$ to the structure of near HFIP gradually formed with increasing HFIP concentration in the range of $x_{HFIP} \geq 0.15$.

III-B-1 Structure and Dynamics of Hexafluoroisopropanol-Water Mixtures by X-Ray Diffraction, Small-Angle Neutron Scattering, NMR Spectroscopy, and Mass Spectrometry

YOSHIDA, Koji[1]; YAMAGUCHI, Toshio[1]; ADACHI, Tomohiro[2]; OTOMO, Toshiya[2]; MATSUO, Daisuke[3]; TAKAMUKU, Toshiyuki[3]; NISHI, Nobuyuki
([1]Fukuoka Univ.; [2]KEK; [3]Saga Univ.)

[*J. Chem. Phys.* **119**, 6132–6142 (2003)]

The structure and dynamic properties of aqueous mixtures of 1,1,1,3,3,3-hexafluoro- 2-propanol (HFIP) have been investigated over the whole range of HFIP mole fraction (x_{HFIP}) by large-angle x-ray scattering (LAXS), small-angle reutron scattering (SANS), ^{19}F-, ^{13}C-, and ^{17}O-NMR chemical shifts, ^{17}O-NMR relaxation, and mass spectrometry. The LAXS data have shown that structural transition of solvent clusters takes place at $x_{HFIP} \sim 0.1$ from the tetrahedral-like hydrogen bonded network of water at $x_{HFIP} \leq \sim 0.1$ to the structure of near HFIP gradually formed with increasing HFIP concentration in the range of $x_{HFIP} \geq 0.15$. The Ornstein- Zernike plots of the SANS data have revealed a mesoscopic structural feature that the concentration fluctuations become largest at $x_{HFIP} \sim 0.06$ with a correlation length of ~ 9 Å, *i.e.*, maximum in clustering and microhetrogeneities. The ^{19}F and ^{13}C chemical shifts of both CF_3 and CH groups of HFIP against x_{HFIP} have shown an inflection point at $x_{HFIP} \sim 0.08$, implying that the environment of HFIP molecules changes due to the structural transition of HFIP clusters. The ^{17}O relaxation data of water have shown that the rotational motion of water molecules is retarded rapidly upon addition of HFIP into water up to $x_{HFIP} \sim 0.1$, moderately in the range of $\sim 0.1 < x_{HFIP} \leq 0.3$, and almost constant at $x_{HFIP} \geq 0.3$, reflecting the structural change in the solvent clusters at $x_{HFIP} \sim 0.1$. The mass spectra of cluster fragments generated in vacuum from HFIP-water mixtures have shown that the predominant clusters are A_1W_n ($n < 12$, A = HFIP, W = water) and water clusters W_n (n = 5–8) at x_{HFIP} = 0.09 and 0.20 and only HFIP oligomers in a water-rich region x_{HFIP} = 0.005 ~ 0.01. From all the information obtained in the present study, the models are proposed for the aggregation of HFIP and water molecules in HFIP-water mixtures.

III-C Ultrafast Dynamics and Scanning Tunneling Microscopy

For the study of molecules on metallic or crystalline surface, very low temperature Scanning Tunneling Microscope (LT STM) system are now in use for collaboration with users in universities. Ultrafast laser systems with pico and femtosecond time resolutions are also available.

III-C-1 Orientation of Adsorbed Nitrous Oxide on Palladium(110) by STM

MATSUSHIMA, Tatsuo[1]; RZEZNICKA, Izabela[1]; WATANABE, Kazuo[2]; INOKUCHI, Yoshiya[2]; NISHI, Nobuyuki
([1]Hokkaido Univ.; [2]Univ. Tokyo)

Adsorbed N_2O on Pd(110) was confirmed to be oriented along the [001] direction at around 8 K by using a low temperature scanning-tunneling microscope, confirming the prediction from angular distributions of desorbing product N_2 in thermal N_2O decomposition and through structure analysis of adsorbed N_2O by density functional theory with generalized gradient approximations. Figure 1 shows a STM image of N_2O-covered Pd(110) at 8 K. Furthermore, the formation of small clusters extended along the [1$\bar{1}$0] direction was first found at low temperatures. These measurements support the reaction mechanism through the N_2O intermediate in catalytic NO_x decomposition.

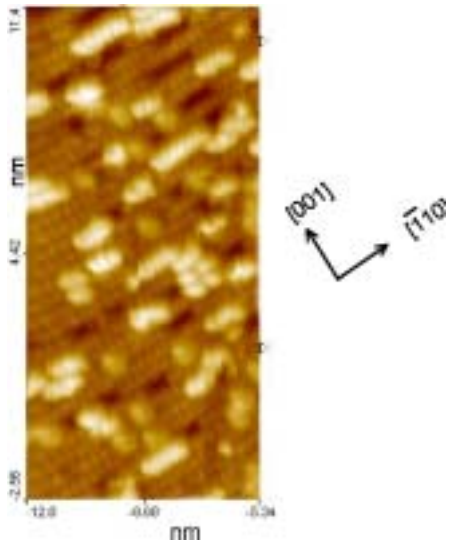

Figure 1. A STM image of N_2O-covered Pd(110) at 8 K. N_2O was dosed at 90–80 K.

III-C-2 Observation of Ultrafast Dynamics of Jet-Cooled *N*-Salicylideneaniline by Femtosecond Time-Resolved REMPI Spectroscopy

OKABE, Chie; NAKABAYASHI, Takakazu[1]; INOKUCHI, Yoshiya[2]; SEKIYA, Hiroshi[3]; NISHI, Nobuyuki
([1]Hokkaido Univ.; [2]Univ. Tokyo; [3]Kyushu Univ.)

[*J. Chem. Phys.* **121**, 9436–9422 (2004)]

N-salicylideneaniline (SA) is well-known photochromic aromatic anil. The excited-state intramolecular proton transfer (ESIPT) followed by photoexcitation of the enol form to its first $^1(\pi,\pi^*)$ state produces the $^1(\pi,\pi^*)$ state of the *cis*-keto form, leading to a metastable *trans*-keto form as the final photoproducts. To investigate ultrafast processes in photoexcited SA, we have applied the femtosecond time-resolved resonance-enhanced multiphoton ionization (REMPI) spectroscopy under the isolated conditions. The decay profile of SA excited at 320 nm is well reproduced by a convolution of the response function with a bi-exponential decay, giving time constants of $\tau_1 < 300$ fs and $\tau_2 = 3.3$ ps. The decay profile of SA measured by varying the pump wavelength from 360 to 373 nm is well fitted using a tri-exponential decay function with time constants of $\tau_1 <$ 300 fs, $\tau_3 = 1.5$ ps, and $\tau_4 > 100$ ps. The difference is attributable to the difference in the ionization efficiency for the enol and keto forms. A very fast decay component ($\tau_1 < 300$ fs) is assigned to a decay of the $^1(\pi,\pi^*)$ state of the enol form. A component $\tau_3 = 1.5$ ps arises from the *cis*-keto form produced *via* the excited-state intramolecular proton transfer (ESIPT) reaction, because the probe wavelength at ~ 400 nm is in resonance with the S_n–S_1 transition of the *cis*-keto form. A component $\tau_2 = 3.3$ ps is attributed to the decay of an excited state of the enol form. The ion signals via the $^1(n,\pi^*)$ state of the enol form as well as the proton-transferred *cis*-keto form emerge within a few hundred femtoseonds after photo-excitation to the first $^1(\pi,\pi^*)$ state of the enol form. This state must be populated *via* the $^1(n,\pi^*)$ state of the enol form, suggesting that an ultrafast non-radiative process occurs in addition to the ESIPT reaction.

Figure 1 shows the deactivation processes following the photoexcitation of the enol form on the basis of the results of the femtosecond time-resolved REMPI measurement together with the theoretical studies. Two ultrafast processes, the ESIPT reaction and an internal conversion (IC) to the $^1(n,\pi^*)$ state, occur on a time scale less than a few hundred femtoseconds from the $^1(\pi,\pi^*)$ state of the enol form. The decay time of the $^1(\pi,\pi^*)$ state of the *cis*-keto form largely changes when the enol form is excited at between 370 and 365 nm. The remarkable change in the decay time is reasonably explained by the existence of a threshold for the ultrafast non-radiative process from the $^1(\pi,\pi^*)$ state of the *cis*-keto form. The opening of an efficient non-radiative channel; an IC from $^1(\pi,\pi^*)$ to $^1(n,\pi^*)$ of the *cis*-keto form promotes the production of the *trans*-keto form as the final photochromic products. The two IC processes provide opposite effect on the quantum yield of photochromic products: IC in the enol form may substantially reduce the quantum yield, but IC in the *cis*-keto form increases it.

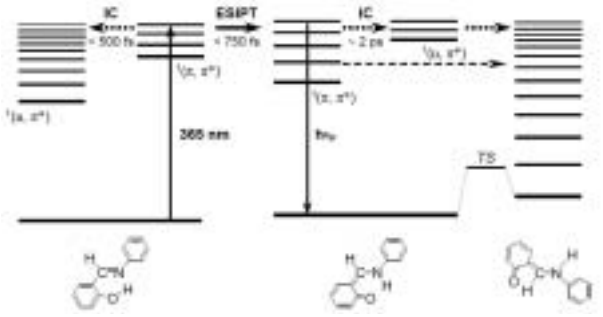

Figure 1. Photoexcited processes of SA drawn on the basis of the femtosecond time-resolved REMPI spectroscopy in gas phase. Two ultrafast processes ESIPT and IC occur by photoexcitation of a high vibronic state of the enol form. When the pump wavelength is shrorter than ~ 365 nm, an IC occurs from the $^1(\pi,\pi^*)$ to the $^1(n,\pi^*)$ state of the proton-transferred cis-keto form in addition to the radiative ($h\nu_F$) and non-radiative decay to the S_0 state. The IC efficiently produces the *trans*-keto form as the final photochromic products. The *trans*-keto form may be produced as a minor channel when the enol form is excited at wavelength longer than 370 nm. *TS* indicates a transition state.

III-C-3 Picosecond Time-Resolved Stokes and Anti-Stokes Raman Studies on the Photochromic Reactions of Diarylethene Derivatives

OKABE, Chie; NAKABAYASHI, Takakazu[1]; NISHI, Nobuyuki; FUKAMINATO, Tuyoshi[2]; KAWAI, Tsuyoshi[2]; IRIE, Masahiro[2]; SEKIYA, Hiroshi[2]
([1]Hokkaido Univ.; [2]Kyushu Univ.)

[*J. Phys. Chem. A* **107**, 5384–5390 (2003)]

The cyclization and cycloreversion reactions of diarylethene derivatives have been studied with picosecond time-resolved Stokes and anti-Stokes Raman spectroscopies. The cyclization reaction of 1,2-bis(2,5-dimethyl-3-thienyl)perfluorocyclopentene (DMTF) is found to occur within 4 ps to produce the vibrationally excited closed forms in the ground electronic (S_0) state. The time constant of the vibrational relaxation toward a thermal equilibrium with solvent molecules is estimated to be about 10 ps. The cycloreversion reaction of 1,2-bis(3,4-dimethyl-5-phenyl-2-thienyl)perfluorocyclopentene (DMPTF) also generates the vibrationally excited open forms in the S_0 state within 4 ps, which decay on a picosecond time scale. The picosecond time-resolved anti-Stokes Raman spectra of DMPTF show two vibrational bands assignable to the C=C stretching modes of the cyclopentene and thiophene moieties of the generated open forms. The Raman intensity arising from the cyclopentene moiety relative to that from the thiophene moiety becomes smaller with the delay time, indicating that part of the excess energy generated *via* the cycloreversion reaction is localized on the C=C stretching mode of the cyclopentene moiety. This result suggests that the C=C stretching mode of the cyclopentene moiety is one of the promoting or the accepting modes in the cycloreversion reaction.

III-D Spectroscopic and Dynamical Studies of Molecular Cluster Ions

Electron defficiency of molecular cluster cations can attract electron rich groups or atoms exhibiting charge transfer or charge resonance interaction in the clusters. This causes dynamical structural change such as proton transfer or ion-core switching in hot cluster ions or clusters in solution.

III-D-1 Structures of $[Mg\cdot(H_2O)_{1,2}]^+$ and $[Al\cdot(H_2O)_{1,2}]^+$ Ions Studied by Infrared Photodissociation Spectroscopy: Evidence of $[HO–Al–H]^+$ Ion Core Structure in $[Al\cdot(H_2O)_2]^+$

INOKUCHI, Yoshiya[1]; OHSHIMO, Keijiro[2]; MISAIZU, Fuminori[3]; NISHI, Nobuyuki
([1]IMS and Univ. Tokyo; [2]RIKEN; [3]Tohoku Univ.)

[*Chem. Phys. Lett.* **390**, 140–144 (2004)]

Infrared spectra of $[Mg\cdot(H_2O)_{1,2}]^+$ and $[Al\cdot(H_2O)_{1,2}]^+$ are measured in the OH stretching region (3200–3800 cm^{-1}). The spectra show the symmetric and asymmetric OH stretching bands of water molecules that are directly bound to the metal ions thorough metal-oxygen intermolecular bonds. In addition to these bands, the $[Al\cdot(H_2O)_2]^+$ ion has another band at 3714 cm^{-1}. This band is assigned to the free OH stretching vibration of the $[HO–Al–H]^+$ ion; the aluminum ion is inserted into the O–H bond of one water molecule in $[Al\cdot(H_2O)_2]^+$.

III-D-2 Infrared Photodissociation Spectroscopy of $[Mg\cdot(H_2O)_{1–4}]^+$ and $[Mg\cdot(H_2O)_{1–4}\cdot Ar]^+$

INOKUCHI, Yoshiya; OHSHIMO, Keijiro; MISAIZU, Fuminori[1]; NISHI, Nobuyuki
([1]Tohoku Univ.)

[*J. Phys. Chem. A* **108**, 5034 (2004)]

Infrared photodissociation spectra of $[Mg\cdot(H_2O)_{1–4}]^+$ and $[Mg\cdot(H_2O)_{1–4}\cdot Ar]^+$ are measured in the 3000–3800 cm^{-1} region. For $[Mg\cdot(H_2O)_{1–4}]^+$, cluster geometries are optimized and vibrational frequencies are evaluated by density functional theory calculation. We determine cluster structures of $[Mg\cdot(H_2O)_{1–4}]^+$ by comparison of the infrared photodissociation spectra with infrared spectra calculated for optimized structures of $[Mg\cdot(H_2O)_{1–4}]^+$. In the $[Mg\cdot(H_2O)_{1–3}]^+$ ions, all the water molecules are directly bonded to the Mg^+ ion. The infrared photodissociation spectra of $[Mg\cdot(H_2O)_4]^+$ and $[Mg\cdot(H_2O)_4\cdot Ar]^+$ show bands due to hydrogen-bonded OH stretching vibrations in the 3000–3450 cm^{-1} region. In the $[Mg\cdot(H_2O)_4]^+$ ion, three water molecules are attached to the Mg^+ ion, forming the first solvation shell; the fourth molecule is bonded to the first solvation shell. As a result, the most stable isomer of $[Mg\cdot(H_2O)_4]^+$ has a six-membered ring composed of the Mg^+ ion, two of the three water molecules in the first solvation shell, and a termination water molecule.